JOURNAL OF MATERIALS SCIENCE 29 (1994) 4764–4770

TEM and high-temperature X-ray diffractometric studies on the structural transformations in Ni_3Al

R. RAMESH*, B. PATHIRAJ‡, B. H. KOLSTER‡
Foundation for Advanced Metals Science (SGM), 7550 KA Hengelo, The Netherlands

High-temperature X-ray diffraction and TEM studies were conducted on nickel-rich boron-doped Ni_3Al in order to confirm our earlier observations on the existence of a structural transformation in these alloys. The results obtained are discussed through a model proposed. The $L1_2$ structure appears to transform to another $L1_2$ or to a DO_{22} structure during heating. Such a transformation starts at around 700 °C and seems to complete around 1100 °C and appears to be of a continuous type. In the temperature range 700–1100 °C both phases coexist, which causes a tetragonal distortion of the $L1_2$ lattice giving rise to a tweed morphology in TEM observations. The transformation mechanism involves a periodic modulation of lattice constant. The calculated values for this periodicity (expressed as a number of unit cells in the [1 0 0] direction) obtained from X-ray diffraction ($L = 62, 70, 74$) matched well with that ($L = 65$) obtained using TEM.

1. Introduction

It is well known that Ni_3Al-based alloys belong to the $L1_2$ kind of ordered structure [1] and it is generally believed that this ordered structure exists as such up to its melting point. However, it has been brought out recently [2, 3] that considerable discrepancies exist in the literature with regard to the long-range order parameter, lattice constants, thermal expansion coefficients and specific heat data of these alloys. It is unusual that in a material which is considered to be stable up to its melting point such irregularities can exist. The discrepancies noticed can be attributed to several reasons. To investigate the possible causes for such variations, a detailed analysis of X-ray diffraction intensity profiles (diffractograms) was carried out at room temperature on filings of stoichiometric and off-stoichiometric Ni_3Al alloys (with and without boron addition) which were annealed over a range of temperatures. This investigation revealed [2] that the $L1_2$ structure in Ni_3Al alloys is not stable at all temperatures, and suggested the existence of a structural transition. Since *in situ* tests always give a better picture of the nature of the transformations involved, the present high-temperature X-ray diffraction study was undertaken on one Ni_3Al alloy, namely a boron-doped nickel-rich composition (76 at % Ni–24 at % Al–0.1 wt % B). Transmission electron microscope (TEM) investigations were also carried out for the same alloy in different heat-treated conditions, to study the changes (if any) in their microstructural behaviour.

2. Experimental procedure

The alloy composition given above was prepared using an induction melting furnace (Heraeus) under a controlled atmosphere of argon and by casting into a copper mould, the details of which are dealt with elsewhere [2]. The high-temperature X-ray measurements were performed over the temperature range from ambient to 1200 °C using an Enraf-Nonius PDS120 integrated powder diffractometry system equipped with an advanced CPS120 curved position-sensitive detector and a high-temperature vacuum chamber operating at approximately 10^{-4} torr vacuum. The sample used was in sheet form, obtained after cold-rolling the ingot several times with intermediate annealing at 1000 °C. The sample was heated by a platinum heating filament and the temperature of the sample was measured using a Pt/Pt–10% Rh thermocouple and was estimated to be accurate within ± 3 °C over the temperature range used. Monochromatic CuK_α radiation was achieved through the use of a curved quartz crystal monochromator. Both cooling and heating sequences of measurement were carried out. The initial condition of the sample was 1200 °C water-quenched. After the room temperature measurement, the sample was heated directly to 1200 °C within 12 min. After obtaining the intensity profiles at 1200 °C, further data collection was made in the sequence of decreasing temperatures in steps of 100 °C down to room temperature. Measurements were then performed likewise in the sequence of increasing temperatures in steps of 100 °C up to 1200 °C. The

Present address: Department of Materials Science and Technology, University of Limerick, Limerick, Ireland.
‡Also with the Faculty of Mechanical Engineering, University of Twente, Enschede, The Netherlands.

0022–2461

residence time at each temperature was 20 min and the cooling/heating rate was 60 °C min^{-1}.

The structural features of the alloy in different heat-treated conditions, namely in 1200, 1000 and 600 °C quenched conditions, were examined in a Jeol 200CX high-resolution TEM operating at 200 kV. Specimens for microstructural examinations were cut from Ni_3Al ingots using a spark erosion machine to a thickness of about 200 μm. Further thinning was done in two stages, first using an electrolyte of 10% HNO_3 in methanol. Discs of about 3 mm diameter were cut from these thin foils and were further jet-polished electrochemically in a solution of 93% methanol and 7% perchloric acid at − 20 °C.

3. Results

3.1. High-temperature X-ray diffraction

Diffractograms obtained during cooling and heating sequences of the sample are shown in Figs 1 and 2 for the fundamental (2 0 0) and superlattice (1 0 0) reflections, respectively. It can be seen in Fig. 1 that at 1200 °C there is no irregularity in the shape of the profile. The order parameter estimated on the basis of an $L1_2$ structure for this temperature using (1 0 0)/(2 0 0) pairs of reflections gave a value of 0.9412 [2] which is fairly close to its theoretical value (0.95) determined for this composition. As the temperature is decreased below 1100 °C an additional peak appears at the right shoulder (higher 2θ) of the first. With a further decrease in temperature, the intensity of the new peak gradually increases at the expense of the original peak and at 800 °C the intensities become almost equal. The intensity of the new peak becomes stronger and at temperatures below 600 °C, the original peak disappears while the new peak continues to become stronger down to room temperature. The changes occurring during cooling are reversed during heating (right-hand figures). However, it is clear that the ratio in intensities of the high to low temperature peaks is higher (at 1000 and 800 °C) during cooling than during heating, indicating that the transformation is an activated process.

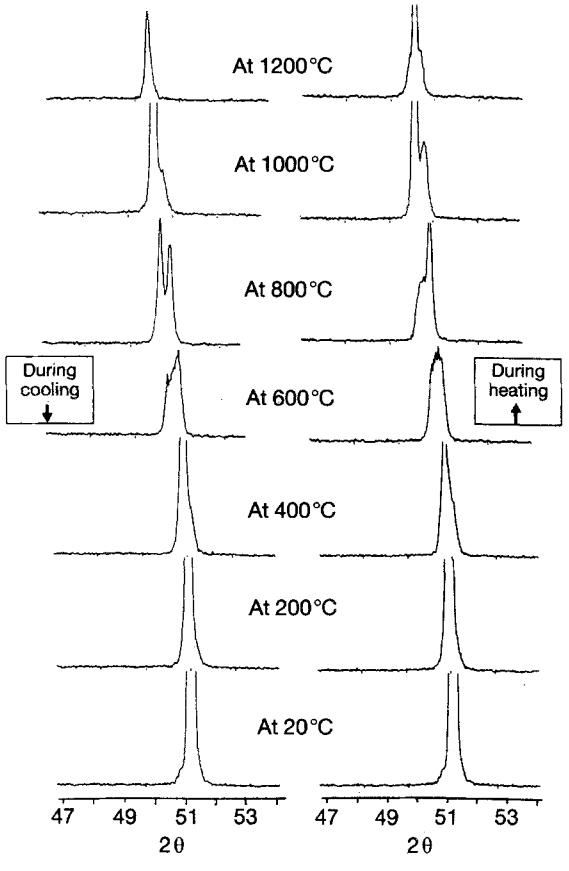

Figure 1 XRD profiles of the (2 0 0) reflection obtained over the range of temperatures for boron-doped off-stoichiometric Ni_3Al during thermal cycling.

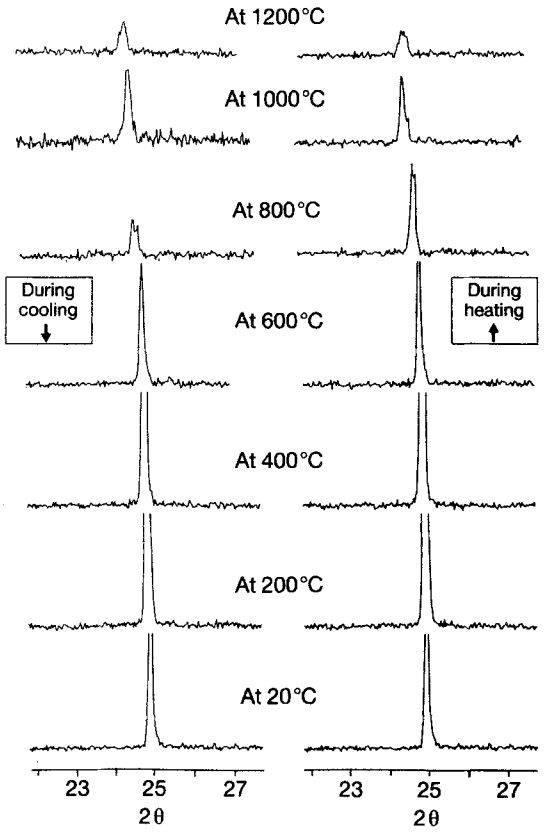

Figure 2 XRD profiles of the (1 0 0) reflection obtained over the range of temperatures for boron-doped off-stoichiometric Ni_3Al during thermal cycling.

The superlattice (1 0 0) profile (Fig. 2) also shows split peaks in the temperature range 800–1000 °C, though they are not so distinct as is the case with the (2 0 0) reflection. The observed shifts in the peak positions for both (2 0 0) and (1 0 0) are purely due to thermal expansion effects.

The lattice parameters were estimated based on (2 0 0) and (1 0 0) reflections. The calculations on the basis of an $L1_2$ structure for the split reflection at 800 °C (during cooling) showed the lattice parameter of the high-temperature phase to be higher by 0.00234 nm as compared with the low-temperature phase. A similar difference in lattice parameter was noticed during the heating cycle when calculated for the well-resolved split peaks seen at 1000 °C. In the following discussions, for the sake of simplicity and convenience the low-temperature and high-temperature phases are designated as $L1_2$(L) and $L1_2$(H), respectively.

Summarizing, the above high-temperature X-ray diffraction results indicate the existence of three regions. It appears that above 1100 °C and below 600 °C the structure is $L1_2$ with the lattice parameter of the latter being smaller than that of the former. In the intermediate region the structures appear to coexist. Though the high-temperature X-ray diffraction results indicate a transition range from 600 to 1100 °C, the actual transition range appears to be from 700 to 1100 °C. The reason for this emerges from additional experiments carried out using dilatometry and calorimetry techniques, the results of which are discussed elsewhere [3].

3.2. TEM investigation

To examine the microstructures in the different transition regions mentioned above, TEM investigations were carried out on samples quenched from 1200, 1000 and 600 °C corresponding to the above-mentioned three regions. With optical microscopy it was not possible to notice any difference between the microstructures obtained for these samples.

Typical TEM microstructural features obtained for the three temperature regions are shown in Fig. 3a–c. The microstructures of the samples quenched from 600 and 1200 °C (Fig. 3a and c) are rather featureless except for the presence of super-dislocations, while those quenched from 1000 °C reveal (Fig. 3b) the features of a strain ("tweed-like") contrast along ⟨1 1 0⟩ in a foil oriented in [0 0 1]. There is also further evidence from the selected-area diffraction patterns that a weak diffuse scattering occurs along all ⟨1 1 0⟩ directions (only a close observation of the negatives of the diffraction patterns shown in Fig. 4 reveals the presence of streaks in the direction of the arrow mark) for the 1000 °C quenched samples, while no such diffuse intensity exists for 600 and 1200 °C quenched ones. The diffuse streaks are similar to those observed in the tweed-like structure of Cu–Be alloys [4] and many other ordering systems which is caused by an order–disorder transition. In order to examine whether the tweed-like morphology exists in the whole intermediate transition range (700–1100 °C), foils of the same alloy quenched from 800 °C were also investigated. A TEM micrograph (Fig. 5) reveals a similar tweed (strain contrast) microstructure oriented along ⟨1 2 3⟩ in the [0 1 3] pattern, indicating the formation of tweed throughout the intermediate range. Since this tweed microstructure is distributed homogeneously throughout the matrix, no significant difference is noticed between the bright-field and the dark-field superlattice images as has been noticed in other systems exhibiting an order–disorder transition [5]. The presence of super-dislocations in the whole temperature range gives a further indication that the structure remains ordered.

4. Discussion

From the *in situ* tests it appears that for temperatures below 700 °C and above 1100 °C an ordered cubic structure of $L1_2$ type exists. The ordered nature of these

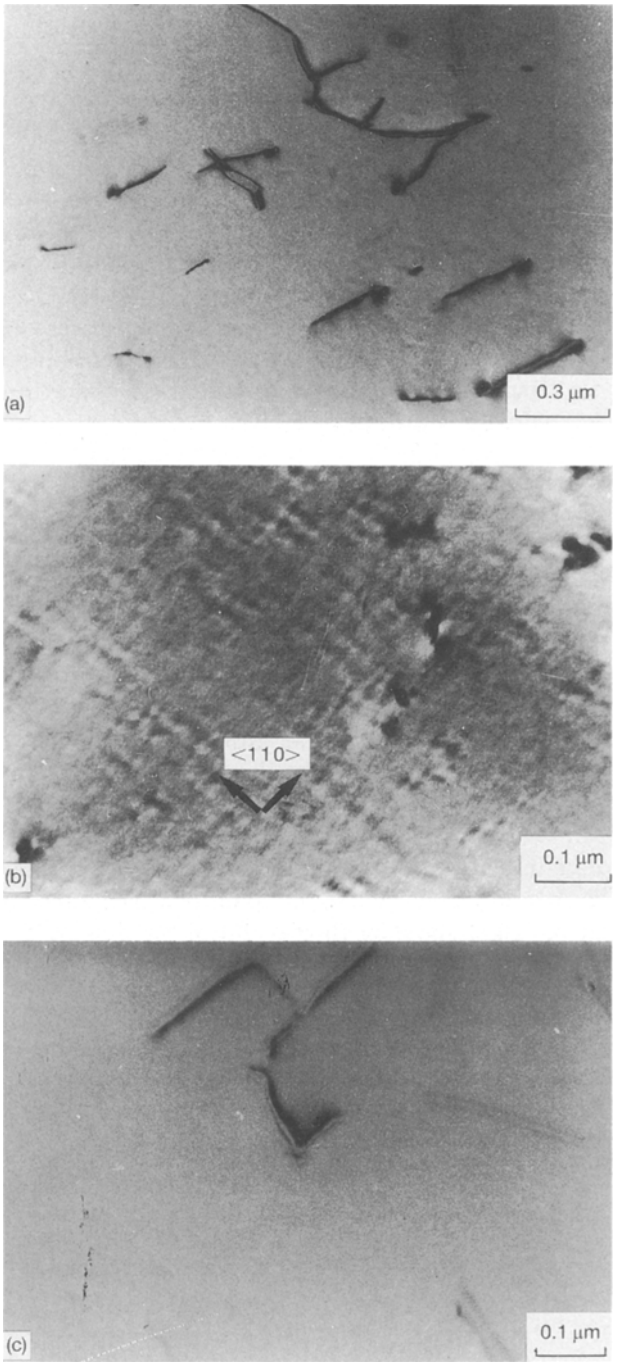

Figure 3 TEM bright-field micrographs of boron-doped nickel-rich Ni_3Al quenched from (a) 600 °C, (b) 1000 °C and (c) 1200 °C. The foils were oriented in [0 0 1] for (a) and (b) and [1 1 1] for (c).

structures was confirmed through the presence of superlattice reflections (Fig. 2). TEM microstructural investigations clearly indicated the presence of super-dislocations (Fig. 3) in these temperature ranges, which further confirms the ordered nature of the structures. However, the cubic structures mentioned in the two regions are not identical as the lattice parameter calculated for the high-temperature structure, $L1_2$(H), was found to be larger by 0.00234 nm as compared to the low-temperature cubic structure $L1_2$(L).

From a physical point of view it remains unclear why there should exist two identical ordered lattices with a difference in lattice parameter only; although

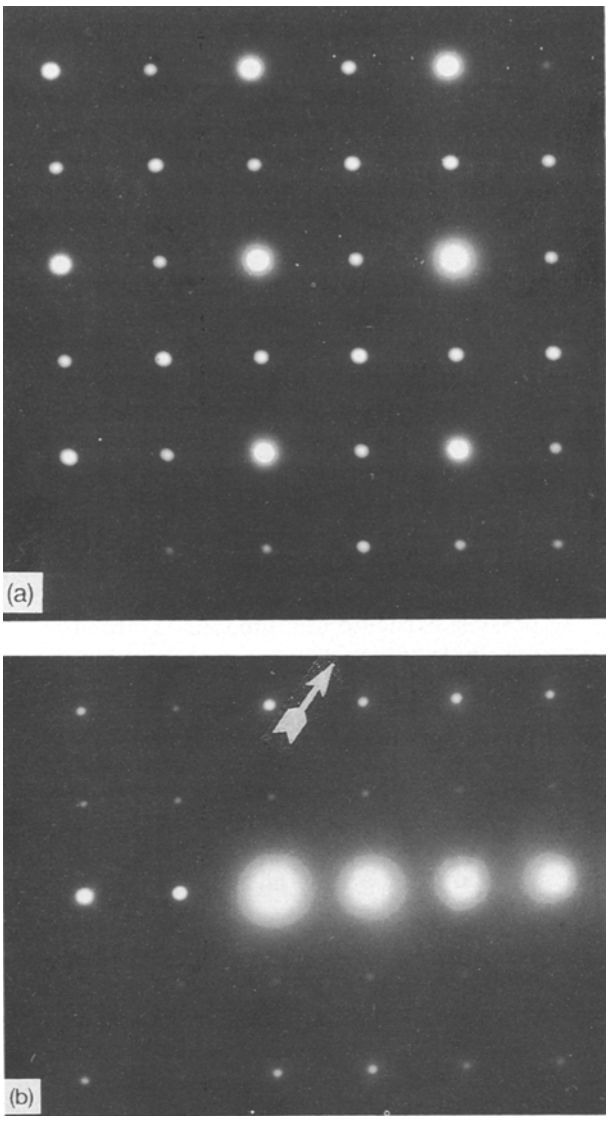

Figure 4 Electron diffraction patterns of Ni_3Al quenched from (a) 600 °C and (b) 1000 °C.

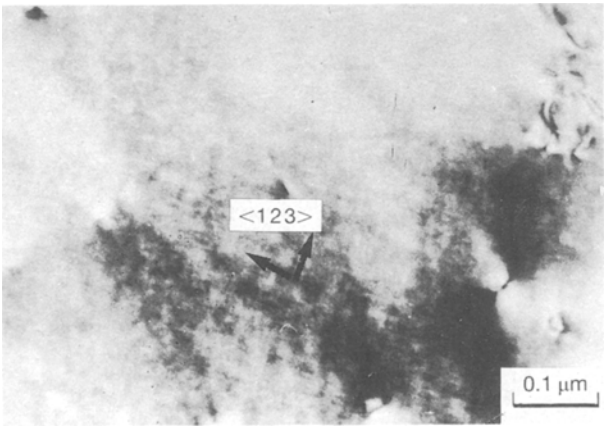

Figure 5 TEM bright-field micrograph of boron-doped nickel-rich Ni_3Al quenched from 800 °C, illustrating the striated contrast along ⟨1 2 3⟩ in the [0 1 3] direction.

this is observed in iron as well, it should be stressed that there the two b.c.c. phases are separated by a stable f.c.c. phase. Therefore, the possible existence of a different phase at high temperatures is also considered. Since a close structural similarity exists between the $L1_2$ and DO_{22} ordered structures, the possibility of DO_{22} being the high-temperature phase is considered and discussed at a later stage. For the sake of discussion, the high-temperature phase is at first assumed to be an $L1_2$-type ordered structure.

Based on the results available, the possible changes that occur in Ni_3Al are discussed through the model proposed below.

4.1. Model

It is postulated above that on either side of the intermediate region (700–1100 °C) the structure is ordered cubic ($L1_2$), with the cell parameter being smaller for the cubic structure that exists below 700 °C, $L1_2$(L), than for the one existing above 1100 °C, $L1_2$(H). Although the in-between temperature range is extended, the high-temperature X-ray diffraction did not give any indication for the existence of a different principal lattice between 700 and 1100 °C. Therefore, in the intermediate region only the transformation takes place and one can expect a mixture of these two different cubic structures:

$$L1_2(L) \rightleftharpoons L1_2(H)$$

This structural change is shown in Fig. 6.

From a mechanistic point of view (not thermodynamically) such a transition might occur through a

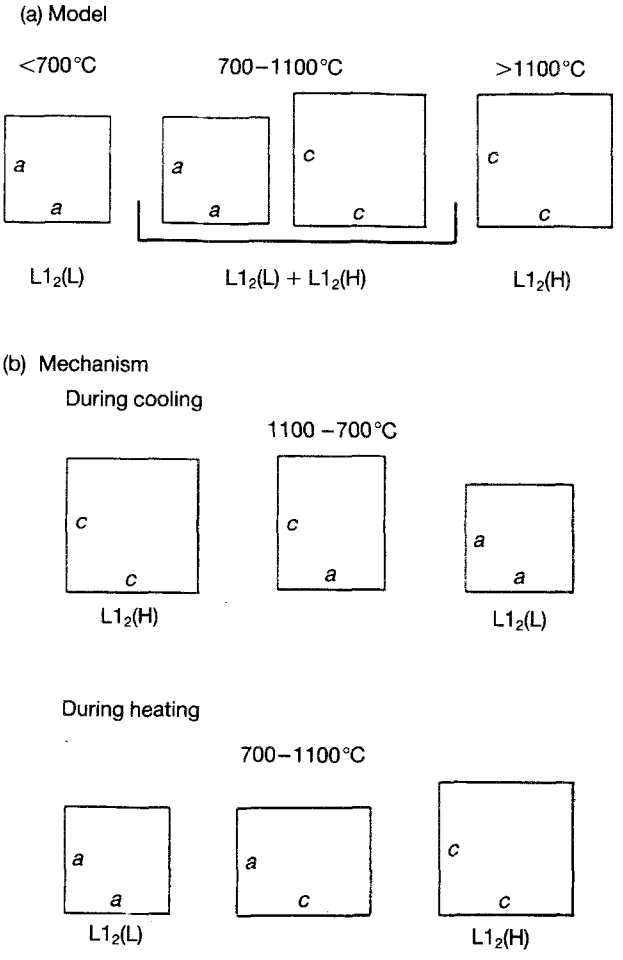

Figure 6 (a) Model describing the proposed structural changes that could possibly exist in Ni_3Al alloys and (b) structural changes from the mechanistic point of view.

metastable state of a localized tetragonal distortion of the lattice. This mechanistic view of the model is shown in Fig. 6b. It predicts the $L1_2(L) \rightleftharpoons L1_2(H)$ transition to occur through a tetragonal distortion of the parent lattice in the intermediate region.

The validity of the proposed model is now considered. The (2 0 0) intensity profiles (Fig. 1) indicate a single peak at 1200 °C corresponding to $L1_2(H)$, and as the sample is cooled through the intermediate temperature range (1100–700 °C) the emergence of an additional peak followed by its increase in intensity at the expense of the original peak is observed. This gives the idea that $L1_2(H)$ is continuously transforming to $L1_2(L)$. Below 600 °C, the original peak disappears and the new peak becomes stronger (due to decreasing thermal scattering effects) until the ambient temperature is reached. This new peak corresponds to $L1_2(L)$. On the other hand, when the sample is heated through the same range, the above process can be seen to reverse with the $L1_2(L)$ peak now becoming weaker at the expense of $L1_2(H)$ beyond 600 °C. From this one can confirm the existence of the $L1_2(L) \rightleftharpoons L1_2(H)$ transition and also the reversibility of the transition.

From Fig. 1 it can be seen that the intensity ratio between the two peaks varies with temperature in the intermediate region. As the multiplicity factors are identical for the two cubic structures, this varying intensity ratio is due to the changing volume fraction of the two phases present during the continuous transformation. Further, from the fact that the unit cell of $L1_2(H)$ is larger than that of $L1_2(L)$, one can make a reasonable assumption that the $L1_2(H) \rightarrow L1_2(L)$ transition (during cooling) occurs more easily compared to the $L1_2(L) \rightarrow L1_2(H)$ transition (during heating). As a consequence of this difference in kinetics, for a given rate of temperature change one can expect different amounts of $L1_2(L)$ and $L1_2(H)$ at any particular temperature in the range 700–1100 °C, depending on whether it is a heating or a cooling cycle. This fits our experimental results (Fig. 1) where the intensity ratio of $L1_2(L)$ and $L1_2(H)$ at any temperature is larger for the heating cycle (compare the differences seen at 800 °C).

The TEM microstructures, which reveal a featureless microstructure except for the presence of superdislocations for samples quenched from 600 and 1200 °C (Fig. 3), indicate the existence of a single-phase ordered structure at a given temperature. For the samples quenched from the intermediate temperature region (Fig. 3b), the microstructures obtained were of unique morphology. The features reveal mottled strain contrast or tweed patterns at many locations in the matrix.

It has been shown that the tweed contrast arises from regular patterns of (invariably) tetragonal strain centres in the parent cubic lattice [6]. The elastic distortions thus resulting due to coherency have been reported to be the primary cause for producing streaks in a sample exhibiting tweed microstructures, as for example in Cu–Be alloys [4], Ni_3V [5] etc. The displacive c → t transformation in the Y_2O_3–ZrO_2 system also exhibits a similar tweed microstructure [7]. In addition to these examples in the other systems, Cheng *et al.* [8] have reported that low-temperature proton irradiation of Ni_3Al produces a mixture of disordered and ordered material, and that the disordered zones which possess the tweed-like morphology are believed to be tetragonally distorted. The existence of a martensitic (tetragonal) phase in binary stoichiometric Ni_3Al prepared by melt-spinning has also been reported [9]. Further, Ni_3Al (γ') precipitates which are the strengthening constituents in Inconel 718 superalloy are believed to undergo a $\gamma' \rightarrow \gamma'_{b.c.t.}$ transformation on the basis of its tweed morphology when aged around 700 °C [10, 11]. However, based on our high-temperature X-ray diffraction study, the existence of a stable tetragonal phase for Ni_3Al can almost certainly be excluded. The probable cause for the observed tweed formation in the intermediate temperature region of the present study can be attributed to the localized strain induced by a periodic modulation.

The possible existence of a modulated structure in the intermediate region is supported by the room-temperature X-ray intensity profiles obtained from the filed samples which were water-quenched from 1000 °C. The experimental details are dealt with in our earlier paper [2]. The intensity profiles indicate the emergence of satellites around the (1 1 1) reflection (Fig. 7). Apparently six satellites, three on the low-angle side and three on the higher-angle side of the

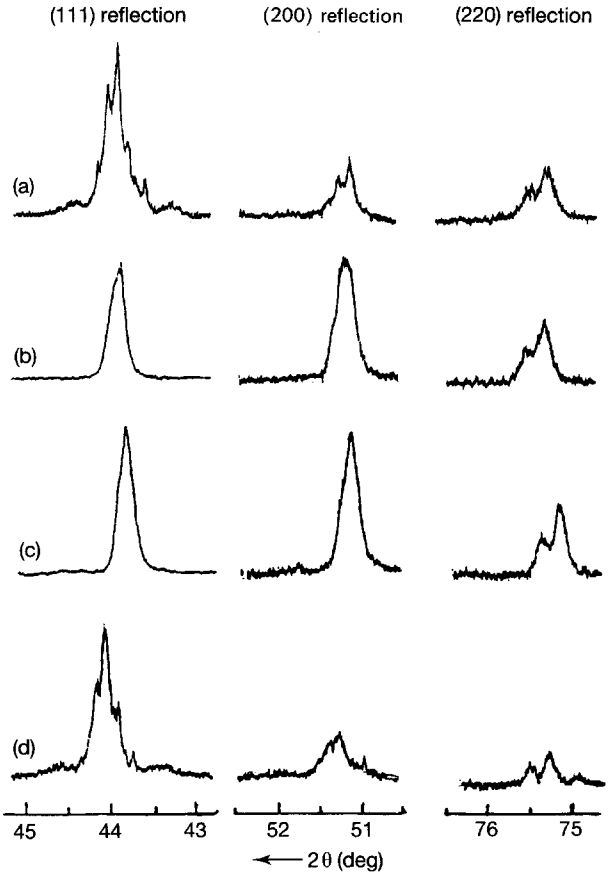

Figure 7 XRD intensity profiles of boron-doped nickel-rich Ni_3Al, providing evidence for the structural transformation at higher temperatures. (a) 1000 °C–24 h, water-quenched; (b) 1000 °C–24 h, water-quenched → 600 °C–2 h; (c) 1000 °C–24 h, water-quenched → 600 °C–12 h; (d) 1000 °C–water-quenched → 600 °C → 1000 °C–water-quenched.

(1 1 1) reflection, are noticed which are symmetrical on either side. Higher-order reflections did not show any satellites, which may be related to their weak intensities. Also the *in situ* high-temperature X-ray diffraction did not reveal such satellites at 1000 °C, and this perhaps is due to the thermal scattering and grain size effect which will be discussed subsequently. The available data were evaluated by means of the Daniel–Lipson relation [12]

$$L = \frac{h \tan\theta}{(h^2 + k^2 + l^2)\delta\theta}$$

where θ is the angle of the Bragg reflection (h,k,l) and $\delta\theta$ the difference in Bragg angle between the centre of a satellite peak and the main line. L is a distance (wavelength of the modulation, i.e. number of subcells in each modulated unit cell) expressed as a number of unit cells in the [1 0 0] direction. The L values estimated based on the (1 1 1) reflection for both 1000 °C–24 h water-quenched (Fig. 7a) and 1000 °C–1 h quenched (Fig. 7d) filings were found to be the same (L = 62, 70 and 74 for the three orders of satellites noticed in both cases). These values are in good agreement with those obtained with TEM, wherein the modulations seen in the micrographs when directly measured on enlarged prints yielded L values in the range 60–65. We believe that these periodic modulations involve modulations of the lattice parameter.

The absence of satellites in the *in situ* high-temperature X-ray diffraction measurements is considered below. In the *in situ* measurements, bulk specimens of rather large grain size (125 μm) were used. This is in contrast to the room-temperature measurements wherein filings of relatively smaller grain size (47 μm) were used [2]. Since the modulations observed are orientation-dependent, the probability of detecting such modulations is greater in the filings than in the bulk specimen, due to the random distribution of the filings. In addition, the thermal scattering effect makes it even more difficult to observe the existence of satellites in the *in situ* measurements.

Summarizing, it can be said that during transformation a cell with a different lattice constant is being formed, which consequently creates mismatch stresses. These are so high that it will not be possible for the two structures to coexist as such. In order to accommodate these stresses the lattice changes gradually from the low- to the high-temperature structure. This creates a modulation with a periodicity comprising 60–70 unit cells. Because of this periodicity satellites are seen. This phenomenon is very much like what one can observe, with spinodal decomposition. It should be pointed out, however, that in the case of spinodal decomposition these modulated structures are due to compositional variations which give rise to strain (lattice constant) modulations, as generally the atomic sizes of the species are not equal. In our case there is no compositional modulation, but only a lattice and thus a strain modulation is present.

Based on the above analysis one can conclude that the transformation mechanism involves a periodic modulation of lattice constant. Such a modulation can be represented schematically as in Fig. 8. Fig. 8a represents modulations involving different lattice constants, i.e. between phases with smaller ($L1_2$(L)) and bigger ($L1_2$(H)) lattice parameters. Due to the coexistence of two phases in the intermediate region, stresses will be invariably developed in the lattice. It is clear that the stresses accompanying the situation in Fig. 8a are much higher than in the situation shown in Fig. 8b. For that reason the existence of an intermediate tetragonal structure as shown in Fig. 8b is more likely than the situation of Fig. 8a. The accommodation of these stresses is reflected as tweed patterns in the TEM features, which indeed indicate a tetragonal distortion. However, the proposed model shows a variation in the [1 0 0] direction whereas from the electron microscopy studies it is clear that the modulation should be in the [1 1 0] direction. This can be simply accounted for by incorporating the variations in lattice parameter in the [1 1 0], rather than in the [1 0 0] direction.

In order to check whether such a mechanism might proceed via a slip process, the following has been tried. The most appropriate slip systems for the atomic $L1_2$ structure have been taken. They are $\{1\,1\,1\}\langle 1\,1\,2\rangle$ and $\{1\,1\,0\}\langle 1\,1\,0\rangle$. Various permutations for the slip systems have been tried and it is found that none of them are possible, as the resulting lattices turn out to be monoclinic and orthorhombic, respectively, which give splitting only in those reflections for which $(h + k)$ is even (h and k are referred to the cubic axes). As Fig. 2 shows a definite splitting of $\{1\,0\,0\}$ where $(h + k)$ is not even, formation of these intermediate structures by slip has to be ruled out.

4.2. Can the high-temperature structure $L1_2$(H) be DO_{22}?

So far in our discussion we have referred to the high-temperature phase as an ordered cubic structure of

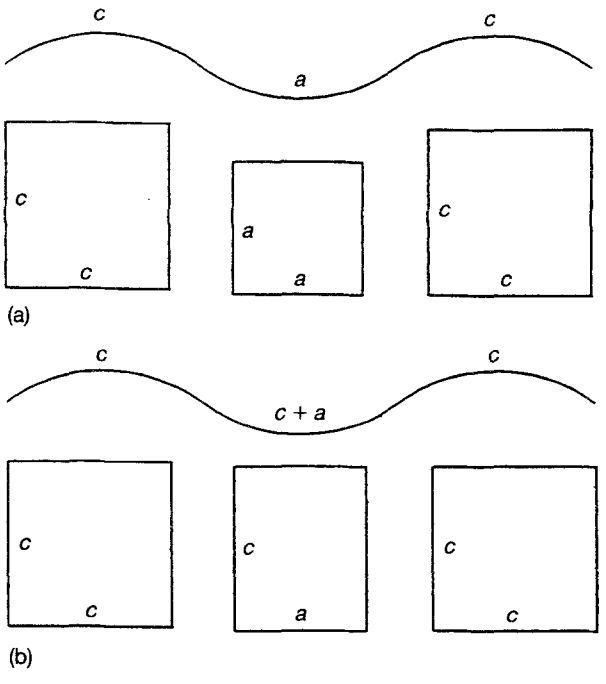

Figure 8 Proposed transformation mechanism in Ni_3Al alloys involving modulations in lattice parameter in the range 700–1100 °C.

$L1_2$ type, and this will now be reviewed. A transition involving the same kind of ordering as $L1_2(L) \rightleftharpoons L1_2(H)$, as discussed in this study, has not been reported so far. As mentioned earlier, the occurrence of a transition of this nature is difficult to understand from a physical point of view. On the other hand, a transition from one ordered to another ordered structure is more likely and a number of such cases have been reported (e.g. the $B_2 \rightleftharpoons DO_3$ transition in the FeAl system [5]). A good structural similarity exists between $L1_2$ and DO_{22} ordered structures. Although a transition between them has been reported only as a likelihood, no experimental confirmation of such a transition exists in the literature.

According to the concept of first neighbour (V_1) and second neighbour (V_2) bond energies, the stable ordered structure will be $L1_2$ type when V_2/V_1 is negative and will be a DO_{22} structure when V_2/V_1 is positive. The tetragonal DO_{22} unit cell is composed of two unit cells of $L1_2$ shifted with respect to each other on the (0 0 1) boundary plane by an amount $\frac{1}{2}a_1 + \frac{1}{2}a_2$, (i.e. by $\frac{1}{2}a$[1 1 0]) as shown in Fig. 9. It is often referred to as "long period" superlattice (one-dimensional) of the $L1_2$ structure with $M = 1$ [13, 14]. In the case of Cu_3Au, Ni_3Al and Ni_3Ga, V_2/V_1 is small as the contribution of V_2 is very small [14, 15] which implies that the $L1_2$ ordered alloy is not in a very stable state and could be influenced easily. Noguchi *et al.* [15] have predicted that an increasing alloying addition can cause an $L1_2$ phase in Ni_3Al alloys to become unstable with respect to DO_{22}. If this is so, it may be quite possible that even the temperature difference can cause the $L1_2$ phase to become unstable with respect to DO_{22}. In such a case, the observed high-temperature phase designated as $L1_2(H)$ can well be a DO_{22} ordered structure. The prerequisite is that it has an a axis little larger than that of $L1_2(L)$ and equal to $\frac{1}{2}c$, in order to fit the XRD results.

More experimental studies involving TEM, single crystals and rigorous thermodynamic analysis would be necessary if unequivocal confirmation of the presence of DO_{22} structure is to be provided.

5. Conclusions

1. It has been established in this study that one and the same $L1_2$ phase in Ni_3Al alloys is not stable at all temperatures.

2. There exist three different phase regions, namely $<700\,^{\circ}C$, 700–1100 °C and $>1100\,^{\circ}C$, in Ni_3Al alloys. The structures are $L1_2(L)$ and $L1_2(H)$ (with the lattice parameter of the latter being larger than that of the former) or DO_{22} (the prerequisite is that it has an a axis little larger than $L1_2(L)$ and equal to $\frac{1}{2}c$) in the $<700\,^{\circ}C$ and $>1100\,^{\circ}C$ temperature regions, respectively. In the intermediate region there is a coexistence of these two structures.

3. The $L1_2(L) \rightarrow L1_2(H)$ or DO_{22} transition is reversible, as revealed by thermal cycling and high-temperature X-ray diffraction studies, and the kinetics appears to be slow.

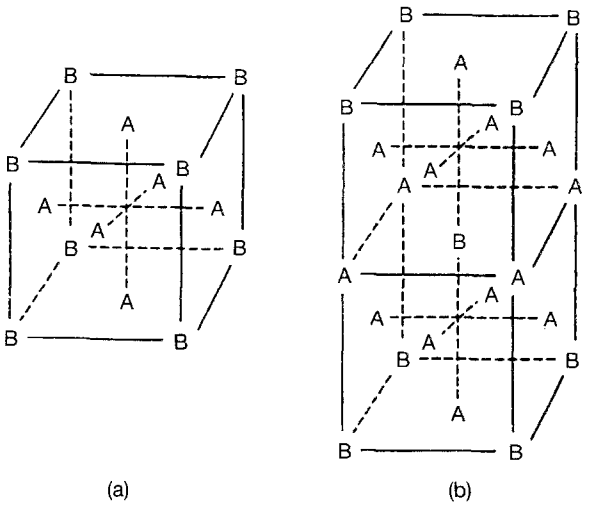

Figure 9 Unit cells of structures of types (a) $L1_2$ and (b) DO_{22}.

4. The transition involves a tetragonal distortion of the parent $L1_2$ lattice and modulations in lattice parameter caused by strain accommodation. The transformation appears to be of a continuous type.

Acknowledgements

The authors thank Enraf-Nonius, Delft for providing the high-temperature facilities and Dr Rudy Visser for his assistance with regard to the measurements.

References

1. M. HANSEN, "Constitution of Binary Alloys" (McGraw-Hill, New York, 1958) p. 119.
2. R. RAMESH, R. VASUDEVAN, B. PATHIRAJ and B. H. KOLSTER, *J. Mater. Sci.* **27** (1992) 270.
3. R. RAMESH, B. PATHIRAJ, J. H. MAAS and B. H. KOLSTER, *Mater. Sci. Engng* **A12** (1992) 60.
4. L. E. TANNER, *Phil. Mag.* **14** (1966) 111.
5. L. E. TANNER and H. J. LEAMY, in Proceedings of International Symposium on Order–Disorder Transformations in Alloys, Tubingen, Germany, 1973, p. 183.
6. P. J. FILLINGHAM, H. J. LEAMY and L. E. TANNER, "Electron Microscopy and Structure of Materials" (University of California Press, Berkeley, 1972) p. 163.
7. A. H. HEUER and M. RUHLE, in Proceedings of 2nd International Conference on Science and Technology of Zirconia, Stuttgart, Germany, 1983, Vol. 12, p. 1.
8. J. CHENG, C. S. LEE, C. N. J. WAGNER and A. J. ARDELL, *MRS Proc.* **113** (1989) 499.
9. K. M. CHANG, S. C. HUANG and A. I. TAUB, *ibid.* **28** (1987) 401.
10. E. L. RAYMOND, *Trans. AIME.* **239** (1967) 1415.
11. R. F. DECKER, in Proceedings of Symposium on Steel Strengthening Mechanisms, Zurich, Switzerland, 1969, p. 1.
12. V. DANIEL and H. LIPSON, *Proc. Roy. Soc. A* **181** (1943) 368.
13. S. C. MOSS and P. C. CLAPP, *Phys. Rev.* **171** (1968) 764.
14. T. SUZUKI, Y. OYA and D. M. WEE, *Acta. Metall.* **28** (1980) 301.
15. O. NOGUCHI, Y. OYA and T. SUZUKI, *Met. Trans.* **12A** (1981) 1647.

Received 13 May 1993
and accepted 8 March 1994